

VU Research Portal

Adsorption energies and ordered structures of hydrogen on Pd(111) from density functional periodic calculations

Løvvik, O.M.; Olsen, R.A.

published in

Physical Review B. Condensed Matter and Materials Physics
1998

DOI (link to publisher)

[10.1103/PhysRevB.58.10890](https://doi.org/10.1103/PhysRevB.58.10890)

document version

Publisher's PDF, also known as Version of record

[Link to publication in VU Research Portal](#)

citation for published version (APA)

Løvvik, O. M., & Olsen, R. A. (1998). Adsorption energies and ordered structures of hydrogen on Pd(111) from density functional periodic calculations. *Physical Review B. Condensed Matter and Materials Physics*, 58, 10890-10898. <https://doi.org/10.1103/PhysRevB.58.10890>

General rights

Copyright and moral rights for the publications made accessible in the public portal are retained by the authors and/or other copyright owners and it is a condition of accessing publications that users recognise and abide by the legal requirements associated with these rights.

- Users may download and print one copy of any publication from the public portal for the purpose of private study or research.
- You may not further distribute the material or use it for any profit-making activity or commercial gain
- You may freely distribute the URL identifying the publication in the public portal ?

Take down policy

If you believe that this document breaches copyright please contact us providing details, and we will remove access to the work immediately and investigate your claim.

E-mail address:

vuresearchportal.ub@vu.nl

Adsorption energies and ordered structures of hydrogen on Pd(111) from density-functional periodic calculations

O. M. Løvvik*

Department of Physics, University of Oslo, P.O. Box 1048 Blindern, N-0316 Oslo, Norway

R. A. Olsen

Theoretische Chemie, Vrije Universiteit, De Boelelaan 1083, 1081 HV Amsterdam, The Netherlands

(Received 6 April 1998)

The full three-dimensional potential energy surface of H on Pd(111) has been calculated with periodic band-structure computations using the generalized gradient approximation of density-functional theory. The fcc hollow site was found to be most stable, followed by the hcp hollow site. Excellent agreement with experimental values of the adsorption energy and the vibrational frequencies was achieved. Subsurface occupation at low coverages and low temperatures is ruled out by our results, but there are no or very low barriers for hydrogen reaching the subsurface region from the molecular gas phase, thus direct absorption is feasible at high coverages. Different ordered structures of the adsorbed hydrogen were considered, and we found that two structures with $\sqrt{3} \times \sqrt{3}R30^\circ$ symmetry are most stable at low temperatures, in agreement with experiment. Results for the adsorption energies and effective hydrogen-hydrogen interactions showed that only fcc hollow sites were occupied on the ordered structures, also in agreement with experiment. [S0163-1829(98)06935-5]

I. INTRODUCTION

Palladium was the first element observed to form a metal hydride, and the palladium-hydrogen system has been thoroughly studied because of its suitability as a hydrogen storage model system.¹⁻⁴ In addition, the interaction of H with Pd surfaces has drawn much attention in connection with hydrogenation catalysis, electrolysis, and hydrogen purification, so there is now a large collection of experimental data and theoretical studies covering the system.^{2,4,5} Hydrogen interacting with low index surfaces of palladium shows a variety of different interesting physical effects, making the system interesting also from a purely academic point of view. There are still some remaining experimental and theoretical ambiguities in the palladium-hydrogen system, and this paper addresses problems concerning subsurface occupation, site preference, and ordered structures of hydrogen at the Pd(111) surface.

It was experimentally established by Conrad *et al.* and Engel and Kuipers that hydrogen easily dissolves into bulk regions of palladium through the densely packed 111 surface.^{6,7} Other experiments by Eberhardt *et al.* indicated the existence of a subsurface site that was irreversibly populated when heating the crystal up to room temperature.^{8,9} In contrast to this, Gdowski and co-workers found that even at low temperatures, regions below the subsurface layer are available for absorption,^{10,11} and another experimental study concluded that subsurface sites probably are energetically more favorable than the surface sites.¹² Felner, Sowa, and Hove quantified this by means of low-energy-electron-diffraction (LEED) measurements and dynamical LEED techniques, and showed that a subsurface to surface occupation fraction of 0–60 % at a temperature of 100 K is consistent with their experiment.¹³

The adsorbed layer of hydrogen on Pd(111) was experimentally examined by means of LEED already by Christ-

mann, Ertl, and Schober, who found that a 1×1 structure is formed at room temperature.¹⁴ The combined experimental and theoretical work by Eberhardt, Louie, and Plummer concluded that this structure is formed by hydrogen populating threefold surface sites.⁹ Felner *et al.*¹⁵ then discovered that at low temperatures two ordered structures with $\sqrt{3} \times \sqrt{3}R30^\circ$ symmetry are found at coverages $\Theta = \frac{1}{3}$ and $\Theta = \frac{2}{3}$. Occupation of the fcc hollow and octahedral subsurface (OSS) sites was shown in a LEED study to be most probable, but hcp hollow site occupation could not be completely ruled out.¹³ (For an explanation and visualization of the different sites, see Fig. 1.) Hsu *et al.*¹⁶ used He scattering, and found C_{3v} symmetry at coverage 1, indicative of one distinct adsorption site. This changed to C_{6v} symmetry when lowering the coverage to $\frac{1}{2}$, and the authors explained this by quantum delocalization at the unit cell level.

Theoretical investigations into the H + Pd(111) system started with semiempirical models. Both the self-consistent pseudopotential mixed-basis calculation of Eberhardt *et al.*⁹ and the embedded atom method (EAM) of Daw and Baskes¹⁷ found a very small energetical difference between the two different hollow sites on the surface. Within the EAM the subsurface sites are energetically just as favorable as the hollow sites on the surface, and the observed $\sqrt{3} \times \sqrt{3}R30^\circ$ symmetry was in this formalism explained by occupation of subsurface sites.^{15,18} This was qualitatively different in the tight-binding model approach by Ezzehar *et al.*¹⁹ They found that the fcc adsorption site is most stable, followed by the OSS site and the hcp site. With increasing machine power and novel computational methods, it has recently become possible to calculate the adsorption energies by using theoretically more advanced methods. Löber and Hennig used the full-potential linear muffin-tin orbital method, and found that the hcp site was most stable, followed by the fcc and OSS sites.²⁰ By employing ultrasoft

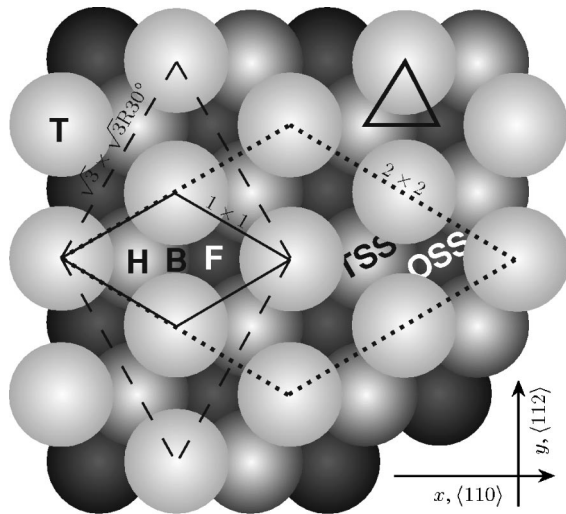


FIG. 1. The surface unit cells considered in this paper: the 1×1 (solid), $\sqrt{3} \times \sqrt{3}R30^\circ$ (dashed), and 2×2 (dotted) surface cells. H and F denote the hcp and fcc threefold hollow sites, respectively (sometimes called the octahedral and tetrahedral surface sites). Directly below the hcp site and above a metal atom in the second layer is the tetrahedral subsurface (TSS) site, and directly below the fcc site and above a metal atom in the third layer is the octahedral subsurface (OSS) site. T is the top site above a surface atom, and B is the bridge site between the fcc and hcp sites. The triangle encloses the minimal region containing all symmetrically unique sites.

pseudopotentials and the local density approximation, Dong *et al.* found that the fcc site is more stable than the hcp site by 60 meV.²¹ Paul and Sautet worked within the generalized gradient approximation of density-functional theory, and found that the hcp site was 170 meV less stable than the fcc site and also 60 meV less stable than the bridge site.²²

Interaction between hydrogen atoms on the Pd(111) surface has been treated theoretically in a number of studies. As already mentioned, Daw *et al.* successfully reproduced the observed $\sqrt{3} \times \sqrt{3}R30^\circ$ ordered structures at low temperatures. In addition to the near degeneracy of the adsorption/absorption sites, the EAM showed no difference between second- and third-nearest-neighbor interaction—it was the postulation of occupation of subsurface sites that led to the correct ordered structure prediction. The embedded cluster calculations of Muscat predicted a 2×2 symmetry of the ordered structure, in conflict with experiments.²³ Ezzehar

et al. used the recursion method in the tight-binding model, and considered occupation of fcc hollow and subsurface octahedral sites.²⁴ They found that the pair interaction between nearest-neighbor fcc sites was attractive, while that between second-nearest-neighbor fcc sites was repulsive. An ordered structure with such properties would exhibit 1×1 symmetry.

This paper deals with the detailed structure of the potential energy surface (PES) of atomic hydrogen at the Pd(111) surface. In Sec. II we present the method used in our calculations. The resulting PES is presented in Sec. III; here we find the preferred adsorption site, calculate the vibrational frequencies, and compare our results with experiments and other theoretical studies. We also study the influence of coverage and lattice relaxations on the adsorption energies. Section IV deals with the interaction between hydrogen atoms at the Pd(111) surface. We first find the energetically preferred ordered structure of chemisorbed hydrogen, and finally we study the effective interaction between hydrogen atoms using a $\sqrt{3} \times \sqrt{3}R30^\circ$ unit cell. Section V concludes.

II. CALCULATIONAL METHOD

We have used the ADF-BAND program^{25,26} to perform total energy calculations of hydrogen adsorbed/absorbed at a three-layer semi-infinite Pd slab with periodicity in two spatial dimensions. Results for both the local density approximation (LDA) and the generalized gradient approximation (GGA) of density-functional theory (DFT) with scalar relativistic effects included through the zeroth-order regular approximation (ZORA) equation can be obtained with this program. We refer to a previous paper for details concerning the program and choice of basis set.²⁷ We showed there that the GGA gave very good results compared to known experimental quantities. The LDA gave both quantitatively and qualitatively different results than seen in experiments, so we use the GGA throughout this paper. We also discussed the number of layers used in the calculations in the previous paper, and found that it is sufficient to use three layers in order to get acceptable results.

We use three different surface unit cells in our calculations: 1×1 , $\sqrt{3} \times \sqrt{3}R30^\circ$, and 2×2 ; all shown in Fig. 1. In order to compare adsorption energies from calculations using different unit cells, it is crucial that our results are properly converged, and we have performed extensive tests to ensure this. Table I shows the largest errors connected with the most important parameters with respect to convergence of the calculations. For the 1×1 surface unit cell they

TABLE I. The table gives the changes in the adsorption energy (E_a) when performing more accurate calculations. KSPACE 5 and 7 (at least 15 and 28 integration points in the irreducible wedge of the surface Brillouin zone) are compared with KSPACE 7 and 9 (at least 28 and 45 integration points), ACCINT 4.5 is compared with 5.0, and the basis set is compared with a basis set with three more Slater-type orbitals (see Ref. 27). The total integration error has been calculated with the assumption that the three error contributions are statistically independent.

	Parameter choice		Maximal error in E_a (meV)			
	KSPACE	ACCINT	KSPACE	ACCINT	Basis sets	Total
1×1	7	4.5	10	5	29	31
$\sqrt{3} \times \sqrt{3}R30^\circ$	5	4.5	34	27	18	47
2×2	5	4.5	10	33	23	41

have been performed on a slab with hydrogen placed in the top-layer plane at the transition state between the fcc and OSS sites, which is quite similar to the geometry with largest errors in Ref. 27. The fcc site has been used to check the convergence of the calculations using the $\sqrt{3} \times \sqrt{3} R30^\circ$ and 2×2 surface unit cells. The ACCINT parameter is a general integration parameter that governs a large number of other parameters related to the real space integration.^{25,26} It is scaled so that the integration accuracy is of the order of $10^{-\text{ACCINT}}$. The KSPACE parameter governs the number of integration points in the surface Brillouin zone. A small surface unit cell gives a large surface Brillouin zone and vice versa, thus smaller surface unit cells need a larger number of points in the k -space integration to obtain the same precision. KSPACE 5 and 7 correspond to at least 15 and 28 integration points in the irreducible wedge of the surface Brillouin zone, respectively. (The number of integration points is dependent on the symmetry of the input geometry.) More integration points mean larger k -space integration accuracy, but also more demanding calculations. The error connected with using a basis set that is smaller than the one giving results close to the basis set limit²⁷ is also given. The total estimated error in the electronic structure calculations is listed in Table I, and we see that in all cases it is below 50 meV.

The optimized lattice constant was previously found to be 3.95 Å at the GGA level,²⁷ but in order to compare more easily with experiments and other theoretical treatments, we have used the experimental value²⁸ of 3.89 Å in our calculations on a rigid lattice.

III. THE PES OF H ON Pd(111)

A. The rigid lattice

The calculations have been performed using three different unit cells on the Pd(111) surface: the 1×1 , $\sqrt{3} \times \sqrt{3} R30^\circ$, and 2×2 unit cells. The surface unit cells and some high symmetry sites are shown in Fig. 1. Since the cost of the calculations strongly depends on the size of the unit cell, we have first calculated the full three-dimensional PES using the 1×1 unit cell, corresponding to coverage $\Theta = 1$. A range of values of the height above the surface z has been calculated for 16 symmetrically unique sites on the surface, corresponding to 54 sites in the 1×1 unit cell. (The symmetrically unique sites lie within the triangle shown in Fig. 1—it spans $\frac{1}{6}$ of the area of the 1×1 cell.) The adsorption/absorption energy of more than 100 different geometries was calculated through

$$E_a = E_{\text{form}}(\text{Pd} + \text{H}) - E_{\text{form}}(\text{Pd}) - \frac{1}{2} E_{\text{bind}}(\text{H}_2), \quad (1)$$

where E_{form} is the formation energy of the hydrogen covered and bare slabs. The binding energy of the hydrogen molecule (E_{bind}) was previously calculated to be -4.80 eV at the GGA level.²⁷ For brevity, we shall simply refer to E_a as the ‘‘adsorption energy.’’ Thus, negative adsorption energies correspond to the adsorbed hydrogen atom being energetically stable with respect to the free hydrogen molecule.

In Fig. 2 the z dependence of the adsorption energy of the four most important sites in the 1×1 surface unit cell is plotted. The adsorption energies at the equilibrium height z_{eq} are listed in Table II, and Fig. 3 shows a two-dimensional cut

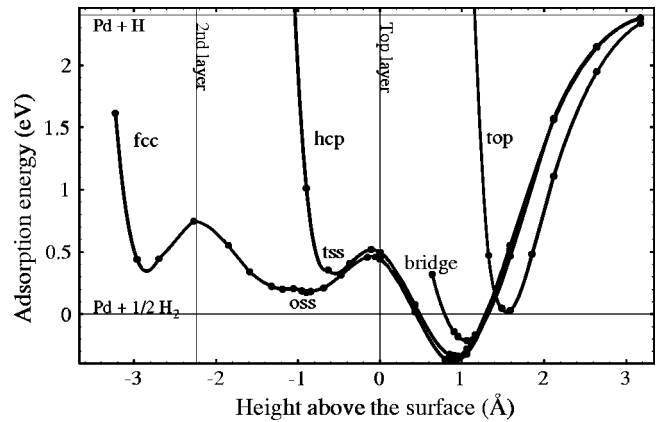


FIG. 2. The adsorption energy (E_a) of some high-symmetry sites as a function of the height above the surface (z) calculated using the 1×1 surface unit cell. The curve marked ‘‘fcc’’ shows the adsorption energy above, at, and below the fcc site, thus also giving the results for the octahedral subsurface (OSS) site and a tetrahedral ‘‘bulk’’ site. The curve marked ‘‘hcp’’ correspondingly gives results for both the hcp and TSS sites. The energy levels corresponding to a hydrogen atom and one of the hydrogen atoms in a hydrogen molecule removed infinitely far from the surface are also marked with lines.

through the full three-dimensional PES for all sites above the surface with the z coordinate restricted to $z = z_{\text{eq}}$. We immediately see that the adsorption energies at the equilibrium heights for the fcc and hcp sites are of the same size, both clearly below the adsorption energy at the equilibrium height for the bridge site. The equilibrium height above the surface is 0.87 and 0.95 Å for the fcc and hcp sites, respectively. This is consistent with the experiment of Felner, Sowa, and Van Hove¹³ who found $z_{\text{eq}} = 0.80 \pm 0.10$ Å with their LEED studies. The fcc site is about 50 meV more stable than the hcp site. The bridge site, midway between the two hollow sites, is approximately 170 meV above the fcc site—this is the barrier to surface diffusion for a rigid lattice. The barrier to subsurface penetration is high and approximately the same for the two sites, about 0.85 eV above the bottom of the surface wells. Considering the experimental findings that hydrogen dissolves through the surface even at low temperatures,¹² we anticipate that surface motion must be important to lower this barrier. We come back to this in Sec. III B. We further see that both the subsurface sites are much higher in energy than the other sites; none of them are stable compared to free molecular hydrogen. We shall see that this is also changed when taking lattice motion into account.

The equilibrium distance between the hydrogen atom and its closest metal atoms varies with the coordination. For a hydrogen atom at the top site, with coordination 1, the equilibrium distance is 1.54 Å. For the bridge site, with coordination 2, the equilibrium distance is 1.73 Å, and for the hcp and fcc sites, both with coordination 3, the equilibrium distances are 1.85 and 1.81 Å, respectively. The TSS site has its equilibrium position close to the geometrical one, and the Pd-H distance here is 1.68 Å. From Fig. 2 we see that the adsorption energy curve is quite flat around the OSS site. The minimum adsorption energy is obtained with $z = -0.90$ Å, corresponding to a distance of 1.82 Å between the H atom and the three closest Pd atoms in the top layer.

TABLE II. The adsorption energies (E_a) in eV at the equilibrium height for different sites as defined in Eq. (1). Our values are compared with some other recent results.

Coverage	This work			BAND ^a		VAMP ^b		VASP ^c	FP-LMTO ^d		Expt. ^e
	1	$\frac{1}{3}$	$\frac{1}{4}$	1	$\frac{1}{3}$	1	$\frac{1}{4}$	$\frac{2}{3}$	1	$\frac{1}{3}$	<0.7
fcc	-0.39	-0.54	-0.44	-0.21	-0.46	-0.43	-0.69	-0.50	-0.30	-0.37	-0.46±0.02
hcp	-0.34	-0.47	-0.41	-0.04	-0.36	-0.37	-0.65	-0.45	-0.32	-0.43	
bridge	-0.21	-0.39	-0.32	-0.10	-0.32	-0.27	-0.41	-0.33	0.01	-0.17	
top	0.02	-0.12		0.37	0.18	0.16	-0.01	0.16			
OSS	0.17	0.02		0.09	-0.15				-0.23	-0.29	
TSS	0.33										

^aADF-BAND DFT calculations within the GGA by Paul and Sautet (Ref. 22). The lattice is rigid, and three and two layers are used for the coverages 1 and $\frac{1}{3}$, respectively.

^bVienna *ab initio* molecular-dynamics program DFT calculations with ultrasoft pseudopotentials within the LDA by Dong *et al.* (Ref. 21). The LDA values have been corrected for half the error in binding energy of the H₂ molecule, 465 meV. The lattice is fully relaxed, and five layers have been used.

^cVienna *ab initio* simulation program DFT calculations with ultrasoft pseudopotentials within the GGA by Dong *et al.* (Refs. 29 and 30). The values are taken from Ref. 30. The lattice is fully relaxed, and five layers have been used.

^dThe full-potential linear muffin-tin orbital method by Löber and Hennig (Refs. 20 and 31). The lattice is relaxed, and seven layers have been used.

^eConrad, Ertl, and Latta (Ref. 6). The coverage was not measured directly, but through the change in the work function.

(The geometrical OSS site is at $z = -1.12$ Å.) There is also a local minimum at $z = -1.19$; then the distance is 1.98 Å to the three closest Pd atoms in the second layer.

The vibrational frequencies were next calculated through simple harmonic fits for the three spatial degrees of freedom of the hydrogen atom, and the results are listed in Table III. At first sight, our results seem to be in quite good agreement with experiment, within 8% of the experimental values if we consider our best numbers. We believe, however, that this is partially fortuitous, since our harmonic fits might be a rather crude approximation. Rick and Doll have shown that anharmonic effects could be important and that the vibrationally excited wave function is nonlocalized—their more thorough calculations using the full periodic Hamiltonian gave lower frequencies than their harmonic approximation.³⁴ Nevertheless, they used the EAM in which the fcc and hcp sites are

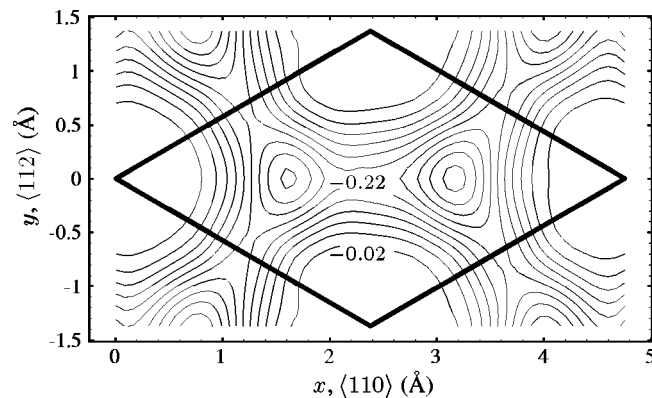


FIG. 3. A contour plot of the adsorption energy based on calculations using the 1×1 surface unit cell. The z coordinate is constrained to be the equilibrium height above the surface, z_{eq} . The contour spacing is 40 meV. The 1×1 surface unit cell is outlined; its corners are placed on top sites.

almost energetically degenerate; this probably makes delocalization more viable. An interesting future study would be to perform similar calculations on a more elaborated PES that does not show the near degeneracy of the hollow sites.

In Fig. 4 we show a comparison of the adsorption energy for coverages 1 and $\frac{1}{3}$ for 12 adsorption sites with $z = z_{\text{eq}}$ along a line connecting two top sites. The adsorption energies of the $\Theta = \frac{1}{3}$ coverage are lowered by 120 and 180 meV compared to the saturated surface, but there are also small qualitative differences. While the top site is the least stable adsorption site for $\Theta = 1$, it has become a local minimum for $\Theta = \frac{1}{3}$, 10 meV lower than the neighboring site. Since our calculations only are converged to within 47 meV, we should be careful not to put too much emphasis on this result, but a local minimum was also found by Dong *et al.*²¹ on a surface with $\Theta = \frac{1}{4}$. This suggests that DFT indeed shows a local minimum in the adsorption energy for the top site at low coverages. We have also calculated the adsorption energy for

TABLE III. The frequencies of the vibrational modes of hydrogen on the Pd(111) surface as calculated by a harmonic fit. Our results are compared with some other theoretical results and with experiment. All the frequencies are measured in cm^{-1} .

Site coverage	This work		Rick, Doll ^a		Expt. ^b
	fcc	hcp	hollow		high ^c
ν_{\perp}	1054	987	884		1000
$\nu_{\parallel x}$	711	715	684	668	
$\nu_{\parallel y}$	686	670	971		774

^aReference 34.

^bReferences 32 and 33.

^cThe coverage was not measured directly, but the hydrogen exposure was 2 langmuirs, and the incidence angle was 57° .

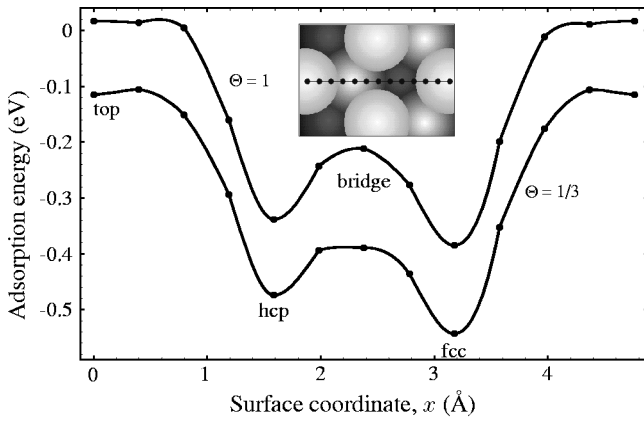


FIG. 4. The adsorption energy along a path connecting two top sites in the $\langle 110 \rangle$ direction (see the inset figure) for the coverages $\Theta = 1$ and $\Theta = \frac{1}{3}$. The z coordinate is constrained to be the equilibrium distance from the surface, z_{eq} .

some of the sites with coverage $\frac{1}{4}$ using a 2×2 surface cell, and the results are summarized in Table II. All our results for the surface with coverage $\Theta = \frac{1}{4}$ are energetically less stable than those for $\Theta = \frac{1}{3}$. This is not surprising, since experiments have found a $\sqrt{3} \times \sqrt{3} R30^\circ$ ordered structure with coverage $\frac{1}{3}$ at low temperatures, and no ordered structures corresponding to $\Theta = \frac{1}{4}$. We shall investigate this further in the next section.

Comparing our results in Table II to Paul and Sautet,²² we find rather large discrepancies, taking into account that we have used the same program. This is most probably due to a bug in the Madelung summation that existed in an older version of the program;^{35,36} we have found quantitatively and qualitatively different results than they even when using the same basis set and integration parameters.

In Ref. 21 the LDA results showed the usual strong overbinding, and the authors found that this was primarily due to the calculated error in binding energy of the H_2 molecule. We have hence used their modified values in Table II, and in this way our results show reasonable agreement. But there are still some discrepancies: all our sites are less stable than theirs, except the top site, which is more stable by 140 and 100 meV ($\Theta = 1$ and $\frac{1}{4}$). The largest difference is for the hollow sites, $\Theta = \frac{1}{4}$, which are both about 250 meV less stable in our calculations than in their modified values. We tried instead to compare the unmodified results of Ref. 21 with our LDA results (not listed in the table), and found that the discrepancies still are there, but to a smaller extent. The largest difference is still for the fcc and hcp sites, $\Theta = \frac{1}{4}$, which now are both about 170 meV less stable in our LDA calculations than in theirs. The discrepancy is still quite large, but this can be caused by the fact that we have used different calculational schemes, a different number of layers, or that their results are given for a fully geometry optimized lattice whereas our results are for a rigid lattice. Two later studies by Dong and co-workers^{29,30} presented GGA calculations of the same system with a coverage $\Theta = \frac{2}{3}$. This is not directly comparable to our results in Table II, but we can see that the trend is still that they get more stable threefold hollow sites and a less stable top site than we do. But in all cases, our results agree on the relative stability of the sites.

The results of Löber and Hennig²⁰ show a slightly differ-

TABLE IV. The effect of relaxation on the adsorption/absorption energies (E_a) for some chosen sites on the surface. Two different types of relaxations are studied: top layer relaxation of the saturated Pd surface ($\Theta = 1$) and in-plane relaxation using the $\sqrt{3} \times \sqrt{3} R30^\circ$ unit cell ($\Theta = \frac{1}{3}$). The adsorption energies of both the rigid (rig.) lattice and the relaxed (rel.) lattice are listed. We have considered four different sites: the fcc hollow, the octahedral subsurface (OSS), the transition state between the fcc and OSS sites (tst—directly below fcc with $z = -0.1$), and the bridge (brg) sites. For the top layer relaxation the outwards relaxation is given both in Å and in % of the bulk interlayer distance, and for the in-plane relaxation only the amplitude of the relaxation coordinate has been given.

	Coverage	Lattice constant a (Å)	Relaxation		E_a eV	ΔE_a meV
			Δx Å	%		
fcc rig.	1	3.95			-0.43	
fcc rel.	1	3.95	0.074	3.2	-0.44	11
OSS rig.	1	3.95			0.00	
OSS rel.	1	3.95	0.25	11.0	-0.13	126
OSS rig.	1	4.14			0.03	
tst rig.	$\frac{1}{3}$	3.89			0.25	
tst rel.	$\frac{1}{3}$	3.89	0.091		-0.04	289
brg rig.	$\frac{1}{3}$	3.89			-0.39	
brg rel.	$\frac{1}{3}$	3.89	0.0		-0.39	0

ent picture than ours; they also find two threefold adsorption sites with approximately the same adsorption energy and the bridge site clearly above the hollow sites, but their results suggest that the hcp site is most stable. Nevertheless, they state in the paper that “almost no differences between the adsorption energies of the two threefold positions can be detected.”²⁰ They found that the OSS site is much more stable than our static results, but they have performed relaxation of the lattice. We shall see in the next section that this is important for the subsurface site.

B. Relaxations

A number of previous calculations have shown that surface motion play an important role in the energetics of hydrogen on surfaces (see, for example, Refs. 18,20 and 21). Since the ADF-BAND program in its current implementation is not capable of calculating forces, all relaxations must be done by hand. This makes full relaxation of all the sites unattainable, and we have to limit the number of geometries to study. We have chosen two different kinds of surface rearrangements: top-layer relaxation for the fcc and OSS sites (to see the effect of relaxations on the adsorption energy on the most stable surface and subsurface sites) and in-plane relaxation for the transition state between the fcc and OSS sites and at the bridge site (to see the effect on the barrier between the surface and subsurface sites and between two surface sites). The results of the calculations are shown in Table IV.

We first consider top-layer relaxation of the surface with hydrogen chemisorbed at the fcc site. To find the energy minimum, we have to compare the lattice with the GGA optimized lattice constant, $a = 3.95$ Å. With this lattice con-

stant, the adsorption energy at the fcc site changes from -0.39 to -0.43 eV for $\Theta=1$. This energy is further decreased by 11 meV when the top layer has an outwards relaxation of 0.074 Å, which is 3.2% of the interlayer separation. We have in our calculations kept the hydrogen-palladium distance constant and varied the distance between the two topmost layers. Löber and Hennig found that the top layer relaxation was 3.5% and 1.0% for the hcp and fcc site, respectively.²⁰

When considering the octahedral subsurface site, the picture is a little bit more complicated. First, the absorption energy of the OSS site is dependent on the lattice constant. If we use the GGA optimized lattice constant for bulk Pd ($a=3.95$ Å), the absorption energy changes from 0.17 to 0.00 eV. In Ref. 27 we found that the optimized lattice constant for palladium hydride is 4.14 Å; the absorption energy of the OSS site with this lattice constant is 0.03. In the calculation of this absorption energy we have used the value of $E_{\text{form}}(\text{Pd})$ with $a=3.95$ Å, since a pure Pd lattice with $a=4.14$ Å is unphysical. With all three lattice constants we found that the preferred distance between the hydrogen atom and the nearest palladium atoms is about 1.8 Å (thus, as already mentioned above, the hydrogen atom is shifted away from the geometrical OSS site). When studying top-layer relaxation for the OSS site we have therefore kept this distance constant and used the GGA optimized lattice constant $a=3.95$. The minimum energy was found for an outward relaxation of 0.25 Å, which is 11% of the interlayer separation; the absorption energy is then -0.13 eV. Löber and Hennig found an outwards relaxation of 6.2%.²⁰ Even though we have found quite large changes in the absorption energy due to lattice relaxations, we have not been able to show that the octahedral subsurface site is as stable as [as predicted by the EAM (Refs. 15 and 18)] or more stable than (as suggested by Eberhardt, Greuter, and Plummer⁸) the fcc hollow site on the surface. It is possible that other kinds of rearrangement of the lattice than considered here could lead to a more stable subsurface site, and that our choice of working with only three layers affects the results. But Löber and Hennig found with the lattice relaxed that the OSS site was at least 90 meV less stable than the fcc site.²⁰ We believe that this supports our results implying that subsurface sites are *not* populated at low temperatures and low coverage. Zero subsurface occupation is consistent with the LEED studies of Felter, Sowa, and Hove.¹³ And, as we will see in Sec. IV A, our results indicate that the $\sqrt{3}\times\sqrt{3}R30^\circ$ phases found by Felter *et al.*¹⁵ can occur without subsurface occupation because of the energy difference between the fcc and hcp sites.

With increasing coverage and temperature, the subsurface sites are going to be accessible by means of further relaxations and thermal motion. But how can our results be consistent with the findings of Gdowski, Stulen, and Felter,¹¹ which showed that hydrogen can penetrate into the lattice at 115 K? To answer this question, we have studied how the activation energy to subsurface penetration is affected by the lattice motion.

We have performed in-plane relaxation of the surface atoms with the hydrogen atom at the transition state from fcc to OSS, which is situated directly below the fcc site with $z=-0.1$ (see Fig. 2). The relaxation is chosen to be a symmetric stretch of the three closest palladium atoms in the

surface plane. We need at least three surface atoms in the unit cell to perform this stretch, and have used the $\sqrt{3}\times\sqrt{3}R30^\circ$ unit cell in our calculations. This relaxation is reminiscent of the stretch involving four surface atoms in our previous study³⁷ considering the effect of surface motion on the direct subsurface absorption of H_2 . The result of the stretching is presented in Table IV: when the three surface atoms each have moved 0.095 Å, the adsorption energy at the transition state has changed to its minimum value of -0.04 eV, down from 0.25 eV. This means that the region below the surface can be reached at low temperatures without any other barrier than the barrier to dissociative adsorption, which is either very low or nonexistent.^{29,30,37} This helps to explain how hydrogen can be found below the surface at 115 K. Gdowski *et al.*¹¹ found that when the surface is saturated with H, further deposition of hydrogen leads to direct absorption of H without equilibration in the chemisorption well. We have shown that the effective barrier to such absorption is low enough to allow for direct absorption at low temperatures. Our simple surface model is not capable of describing how hydrogen goes further into the metal and how the hydride phase is created, but the low barrier to direct subsurface penetration makes our results compatible with Ref. 11.

We have also studied in-plane relaxation of the bridge transition state, but as shown in Table IV, no relaxation could be found. We considered a symmetric stretch of the two closest metal atoms, and we first tried to keep the hydrogen-metal distance constant and then the height of the hydrogen atom above the surface constant. Dong *et al.* did not find any relaxation of the bridge site either.²¹ This means that the barrier to surface diffusion should be about 170 meV (not including zero-point energy effects) at the relaxed surface as well.

We have not considered any other relaxations, although there are surely more to find. For example, Dong *et al.* found that hydrogen placed at sites between the hollow sites and the top site provoked a relaxation of the top-layer *parallel* to the surface.²¹ Taking this into account would lower some of the sites near the hollow sites, and thus lower the frequency of the parallel vibrations. Apart from this, we believe that we have found the most important effects of surface rearrangements on the energetics of our simple system, namely the changes in adsorption energies of the most stable surface and subsurface sites and the changes in diffusion barriers on the surface and down to the subsurface site.

IV. HYDROGEN-HYDROGEN INTERACTIONS

A. Different coverages

In the preceding section we saw that the adsorption energy depends on the coverage. The experimental findings of Conrad, Ertl, and Latta did not show such a dependency; they found that the adsorption energy was -0.456 ± 0.022 eV per hydrogen atom in the whole region covered by the experiment.⁶ The molecular-beam experiment of Engel and Kuipers did, however, find some evidence that the adsorption energy varied, and found by using a simple model that E_a varied from -0.47 eV at low coverages to -0.39 eV at high coverages.⁷ The latter experiment was performed at temperatures of 250 K and above, while our

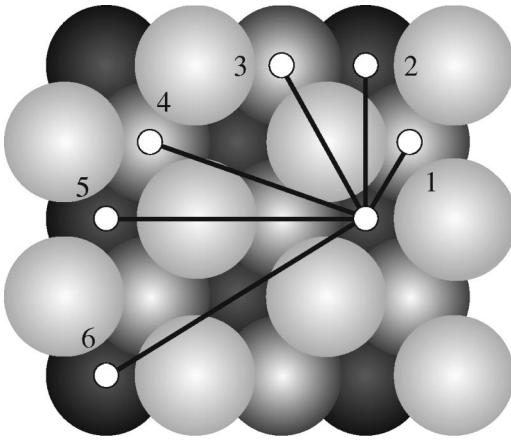


FIG. 5. The six nearest neighbors of an fcc site when both fcc and hcp sites are considered. If only fcc sites were considered, the three nearest fcc neighbors would correspond to our second, fifth, and sixth nearest neighbors. The 1×1 , 2×2 -2H, $\sqrt{3} \times \sqrt{3}R30^\circ$ -1H, and 2×2 -1H ordered structures are made up of second, third, fifth, and sixth nearest neighbors, respectively.

calculations are at zero temperature. We do not know of any experiment measuring the adsorption energy for H on Pd at lower temperatures, where the ordered $\sqrt{3} \times \sqrt{3}R30^\circ$ structures appear.

Since we are only able to calculate the adsorption energy using periodic structures, we do not get out the effective two-particle interactions of the hydrogen atoms without the use of unattainably large surface unit cells. We are, however, able to directly compare the stability of different ordered structures, and through this make comparisons of some different multiparticle interactions. Figure 5 shows the nearest neighbors of an atom placed at an fcc site. To be able to describe different kinds of ordered structures, we take into account both the fcc and hcp sites; thus the second, fifth, and sixth nearest neighbors correspond to the nearest, next nearest, and third nearest fcc sites, respectively.

We have calculated the adsorption energy of some different ordered structures, and plotted it as a function of coverage in Fig. 6. The adsorption energy for coverage 1 has been

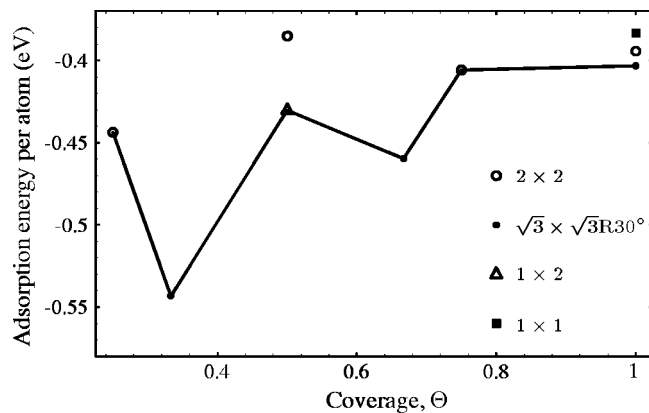


FIG. 6. The adsorption energy per hydrogen atom as a function of the coverage for different ordered structures. The circles, points, triangle, and rectangle designate 2×2 , $\sqrt{3} \times \sqrt{3}R30^\circ$, 1×2 , and 1×1 ordered structures, respectively. The 1×2 ordered structure has been calculated by using the 2×2 surface unit cell.

TABLE V. Ordered structures of H on Pd(111) that have been studied. The adsorption energy is per hydrogen atom.

Structure	Θ	Nearest neighbor	Number of neighbors	Adsorption energy (eV)
1×1	1	2nd	6	-0.40
1×2	$\frac{1}{2}$	2nd	2	-0.43
$\sqrt{3} \times \sqrt{3}R30^\circ$ -1H	$\frac{1}{3}$	5th	6	-0.54
$\sqrt{3} \times \sqrt{3}R30^\circ$ -2H	$\frac{2}{3}$	2nd	3	-0.46
$\sqrt{3} \times \sqrt{3}R30^\circ$ -4H	$\frac{4}{3}$	1st	3	-0.14
2×2 -1H	$\frac{1}{4}$	6th	6	-0.44
2×2 -2H	$\frac{1}{2}$	3rd	3	-0.39
2×2 -3H	$\frac{3}{4}$	2nd	4	-0.41

calculated using all three unit cells, and we see that it varies with less than 20 meV; this shows that it is meaningful to compare results using the different unit cells. The smallest coverage that we have calculated is $\frac{1}{4}$, constructed by sixth nearest neighbors. The distance between the hydrogen atoms is then 5.5 Å, and we should expect the hydrogen interaction to be quite small at this distance. We see that two of the structures in Fig. 6 are more stable than this, namely the two $\sqrt{3} \times \sqrt{3}R30^\circ$ structures. Our calculations thus predict that those structures should be favored at low temperatures, in accordance with experiment.¹⁵ Felter *et al.* obtained more or less the same results as we did with the EAM, but they found that the 1×2 and both the $\sqrt{3} \times \sqrt{3}R30^\circ$ structures all were equally stable.^{15,18} Since they also found that four different sites were energetically nearly degenerate (fcc, hcp, OSS, and TSS), they had to postulate subsurface occupation and use equilibrium Monte Carlo simulations to recreate the experimentally observed ordered structures.

We want to discuss the pair- and many-particle interactions in more detail, and have listed results for some of the calculated structures in Table V. We take as our starting point the 2×2 -1H structure with $\Theta = \frac{1}{4}$. For the sake of comparison, we define for now the interaction at this distance (5.5 Å) to be zero. We first note that of the four ordered structures composed of second nearest neighbors, the 1×1 structure is the least stable. This structure has the largest number of neighbors, suggesting that the second-nearest-neighbor interaction is repulsive. But we have already seen that the $\sqrt{3} \times \sqrt{3}R30^\circ$ -2H structure ($\Theta = \frac{2}{3}$) is more stable than our low coverage limit, indicating that this structure consists of attractive interactions. Since this structure is also constructed of second nearest neighbors, it is thus not enough to know the two-particle interactions to predict stable periodic structures. Nevertheless, a comparison of the other ordered structures should at least reveal some clues about how the pair- and many-particle interactions are related. The 2×2 -2H structure ($\Theta = \frac{1}{2}$) is built up of third nearest neighbors; thus every second occupied site must be a hcp site. We see that this structure is relatively unstable, but this is primarily due to the less stable hcp site. If we compensate for the hcp site being about 50 meV less stable than the fcc site, we find that the effective third-nearest-neighbor interaction is almost zero compared to our low coverage limit. Of all the ordered structures, the $\sqrt{3} \times \sqrt{3}R30^\circ$ -1H ($\Theta = \frac{1}{3}$) is by far the most stable. It is constructed by fifth nearest neighbors,

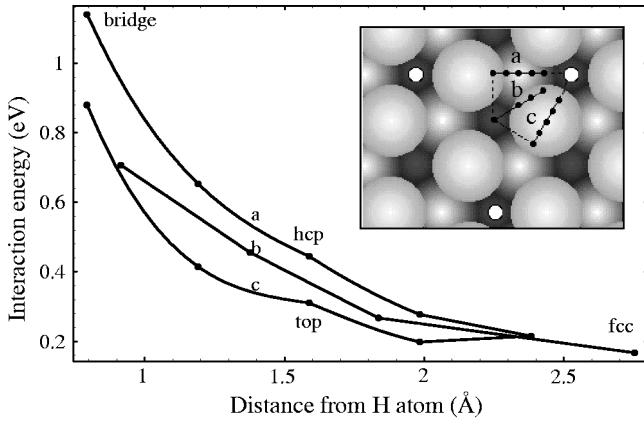


FIG. 7. The interaction energy E_{int} [defined in Eq. (2)] between a H atom placed at the fcc site and a second hydrogen atom placed in a $\sqrt{3} \times \sqrt{3} R 30^\circ$ unit cell. The inset figure shows the geometries; the white disks are the H atoms at the fcc sites, whereas the points are the positions of the second atom. We have plotted points along three directions, marked by ‘‘a,’’ ‘‘b,’’ and ‘‘c.’’ All symmetrically unique sites lie within the region enclosed by the lines marked by ‘‘a’’ and ‘‘c,’’ and the dashed lines.

so our results suggest that the fifth-nearest-neighbor interaction is quite attractive. If we compare these results with Ezzehar *et al.*,²⁴ we find quite large differences. They used the tight-binding method, and found that the fifth-nearest-neighbor pair interaction was repulsive, while the second-nearest-neighbor interaction was found to be attractive by more than 100 meV.²⁴ This was independent of surface or subsurface occupation, and the same trend was observed when they considered trimer and tetramer interactions. Their results are thus consistent with a 1×1 ordered structure. Our results show an attractive fifth-nearest-neighbor interaction and a repulsive second-nearest-neighbor interaction, with the $\sqrt{3} \times \sqrt{3} R 30^\circ$ -2H structure as an exception of the latter—we have thus predicted both the experimentally observed $\sqrt{3} \times \sqrt{3} R 30^\circ$ structures with our adsorption energy calculations.

B. Interactions on the $\sqrt{3} \times \sqrt{3} R 30^\circ$ unit cell

We now turn to the detailed structure of the hydrogen-hydrogen interaction on the $\sqrt{3} \times \sqrt{3} R 30^\circ$ surface cell. We have calculated the adsorption energy for a number of configurations with $\Theta = \frac{2}{3}$ and one of the H atoms placed at the fcc site. By comparing configurations with and without a second H atom, we have found the interaction energy defined as

$$E_{\text{int}} = E_a(\text{Pd} + \text{H}_I + \text{H}_{II}) - E_a(\text{Pd} + \text{H}_I) - E_a(\text{Pd} + \text{H}_{II}), \quad (2)$$

where $E_a(\text{Pd} + \text{H}_I + \text{H}_{II})$ is the adsorption energy for two hydrogen atoms (H_I and H_{II}) adsorbed on the slab, and $E_a(\text{Pd} + \text{H}_I/\text{H}_{II})$ is the adsorption energy for one hydrogen atom (H_I/H_{II}) adsorbed on the slab. H_I is always placed at the fcc site, and H_{II} is placed at one of the sites shown in the inset figure of Fig. 7. E_{int} thus gives a measure of the effective interaction between two H atoms compared to the most stable structure, $\sqrt{3} \times \sqrt{3} R 30^\circ$ -1H.

In Fig. 7 we have shown some of the resulting interaction energies. We see that the effective interaction is the largest along the ‘‘a’’ path, which is across the bridge and towards the hcp sites. When heading towards the top site (path ‘‘c’’), the interaction is the smallest. Studying the electron charge of the adsorbed hydrogen atom, which is lowest at the top site and highest at the fcc site, we see the following trends. All the sites along curve ‘‘a’’ have higher electron charges on the hydrogen atom than the sites along curve ‘‘c,’’ suggesting a larger electrostatic repulsion between the hydrogen atoms when considering sites along curve ‘‘a.’’ The electron charges on the hydrogen atoms on the sites along curve ‘‘b’’ lie between those for curve ‘‘a’’ and ‘‘c,’’ and as we see from Fig. 7, the interaction energies along curve ‘‘b’’ also lie in the middle. We further see that placing H_{II} at another fcc site gives the lowest interaction, about 160 meV. This agrees with the difference of 80 meV per atom between the two $\sqrt{3} \times \sqrt{3} R 30^\circ$ structures that can be read out from Table V or Fig. 6. Two other sites have almost just as low E_{int} as the fcc site, but they have such high adsorption energies that they are improbable to populate. The interaction energy of the hcp site is almost 0.5 eV, thus ruling out first-neighbor occupation.

Since the fcc site is most stable, the best way of placing two atoms in the $\sqrt{3} \times \sqrt{3} R 30^\circ$ unit cell is in two fcc sites. We have also considered other possibilities, such as placing one of the atoms subsurface and the other in a fcc or hcp site, but since the subsurface sites are so much higher in energy, all these possibilities are much less stable than the configuration with two fcc sites. We conclude that our results clearly imply that two fcc sites should be occupied in the $\sqrt{3} \times \sqrt{3} R 30^\circ$ unit cell when the coverage is $\frac{2}{3}$. Subsurface occupation at low temperatures is ruled out at this coverage.

The details of the hydrogen interaction would be of importance in a dynamical study of hydrogen diffusion on the Pd(111) surface, and we have work in progress on this subject.³⁸

V. CONCLUSIONS

We have used periodic density-functional calculations within the generalized gradient approximation to investigate in detail the potential energy surface (PES) of hydrogen atoms at the Pd(111) surface. We have constructed the full three-dimensional PES using a 1×1 surface unit cell (coverage $\Theta = 1$), and in addition calculated the adsorption energies at the equilibrium geometries for some sites using the $\sqrt{3} \times \sqrt{3} R 30^\circ$ and 2×2 surface unit cells (coverages $\Theta = \frac{1}{3}$ and $\frac{1}{4}$). We found that the fcc hollow site is preferred, with an adsorption energy varying with coverage from -0.54 to -0.39 eV. The hcp hollow site is between 40 and 70 meV less stable, and the bridge site between the hollow sites is from 140 to 170 meV above the fcc site. Outward relaxation of the palladium top layer lowered the adsorption energy at the fcc site by 11 meV. The subsurface sites were not found to be stable compared to free molecular hydrogen on the rigid surface, but relaxation of the surface lowered the adsorption energy of the octahedral subsurface site to -0.13 eV. The low stability of the octahedral subsurface site as compared to the fcc site rules out subsurface occupation at low temperatures and low coverages. But surface mo-

tion makes the region below the surface available directly from the molecular gas phase without any other barriers than the possible barrier to dissociative adsorption—this means that direct absorption of hydrogen is possible at high coverages. Our harmonic fit to the PES gave a perpendicular vibrational with frequency 1054 cm^{-1} , and two parallel frequencies of 711 and 686 cm^{-1} , in good agreement with experiment.³²

To study the hydrogen-hydrogen interaction we calculated the adsorption energy of hydrogen atoms using different periodic structures, and found that two ordered structures with $\sqrt{3} \times \sqrt{3}R30^\circ$ symmetry are preferred at zero temperature, in accordance with experiment.¹⁵ We also studied the interaction between hydrogen atoms using the $\sqrt{3} \times \sqrt{3}R30^\circ$ surface unit cell, and the results suggest that the effective hy-

drogen interaction energy is sensitive to the bonding coordination of the hydrogen; the higher coordination, the higher repulsion. We found that the ordered structures with $\sqrt{3} \times \sqrt{3}R30^\circ$ symmetry have all the hydrogen atoms located at fcc sites.

ACKNOWLEDGMENTS

We thank Pier Philipsen for valuable discussions, Evert-Jan Baerends for his comments on the manuscript, and Jørn Amundsen for his outstanding computer support. The calculations have been carried out under a grant of computer time by the Norwegian Research Council. The authors were also financed by the Norwegian Research Council.

*Electronic address: o.m.lovvik@fys.uio.no

- ¹W. M. Mueller, J. P. Blackledge, and G. G. Libowitz, *Metal Hydrides* (Academic Press, New York, 1968).
- ²*Hydrogen in Metals*, edited by G. Alefeld and J. Völkl (Springer-Verlag, Berlin, 1978).
- ³Y. Fukai, *The Metal-Hydrogen System* (Springer-Verlag, Berlin, 1993).
- ⁴*Hydrogen in Metals III. Properties and Applications*, edited by H. Wipf (Springer-Verlag, Berlin, 1997).
- ⁵K. Christmann, Surf. Sci. Rep. **9**, 1 (1988).
- ⁶H. Conrad, G. Ertl, and E. E. Latta, Surf. Sci. **41**, 435 (1974).
- ⁷T. Engel and H. Kuipers, Surf. Sci. **90**, 162 (1979).
- ⁸W. Eberhardt, F. Greuter, and E. W. Plummer, Phys. Rev. Lett. **46**, 1085 (1981).
- ⁹W. Eberhardt, S. G. Louie, and E. W. Plummer, Phys. Rev. B **28**, 465 (1983).
- ¹⁰G. E. Gdowski, T. E. Felter, and R. H. Stulen, Surf. Sci. Lett. **181**, L147 (1987).
- ¹¹G. E. Gdowski, R. H. Stulen, and T. E. Felter, J. Vac. Sci. Technol. A **5**, 1103 (1987).
- ¹²G. D. Kubiak and R. H. Stulen, J. Vac. Sci. Technol. A **4**, 1427 (1986).
- ¹³T. E. Felter, E. C. Sowa, and M. A. Van Hove, Phys. Rev. B **40**, 891 (1989).
- ¹⁴K. Christmann, G. Ertl, and O. Schober, Surf. Sci. **40**, 61 (1973).
- ¹⁵T. E. Felter, S. M. Foiles, M. S. Daw, and R. H. Stulen, Surf. Sci. Lett. **171**, L379 (1986).
- ¹⁶C.-H. Hsu, B. E. Larson, M. El-Batanouny, C. R. Willis, and K. M. Martini, Phys. Rev. Lett. **66**, 3164 (1991).
- ¹⁷M. S. Daw and M. I. Baskes, Phys. Rev. B **29**, 6443 (1984).

- ¹⁸M. S. Daw and S. M. Foiles, Phys. Rev. B **35**, 2128 (1987).
- ¹⁹H. Ezzehar, L. Stauffer, and H. Dreyssé, Z. Phys. Chem. (Munich) **181**, 305 (1993).
- ²⁰R. Löber and D. Hennig, Phys. Rev. B **55**, 4761 (1997).
- ²¹W. Dong, G. Kresse, J. Furthmüller, and J. Hafner, Phys. Rev. B **54**, 2157 (1996).
- ²²J. F. Paul and P. Sautet, Phys. Rev. B **53**, 8015 (1996).
- ²³J.-P. Muscat, Phys. Rev. B **33**, 8136 (1986).
- ²⁴H. Ezzehar, L. Stauffer, H. Dreyssé, and M. Habar, Surf. Sci. **331-333**, 144 (1995).
- ²⁵G. te Velde and E. J. Baerends, Phys. Rev. B **44**, 7888 (1991).
- ²⁶G. te Velde and E. J. Baerends, J. Comput. Phys. **99**, 84 (1992).
- ²⁷R. A. Olsen *et al.*, J. Chem. Phys. **106**, 9286 (1997).
- ²⁸C. Kittel, *Introduction to Solid State Physics*, 6th ed. (Wiley, New York, 1986).
- ²⁹W. Dong, G. Kresse, and J. Hafner, J. Mol. Catal. A: Chem. **119**, 69 (1997).
- ³⁰W. Dong and J. Hafner, Phys. Rev. B **56**, 15 396 (1997).
- ³¹R. Löber, Ph.D. thesis, Humboldt University of Berlin, 1995.
- ³²H. Conrad, M. E. Kordesch, R. Scala, and W. Stenzel, J. Electron Spectrosc. Relat. Phenom. **38**, 289 (1986).
- ³³H. Conrad, M. E. Kordesch, W. Stenzel, and M. Sunjic, J. Vac. Sci. Technol. A **5**, 452 (1987).
- ³⁴S. W. Rick and J. D. Doll, Surf. Sci. Lett. **302**, L305 (1994).
- ³⁵P. Sautet and J. F. Paul (private communication).
- ³⁶G. Wiesenekker, G. J. Kroes, E. J. Baerends, and R. C. Mowrey, J. Chem. Phys. **103**, 5168 (1995).
- ³⁷R. A. Olsen, G. J. Kroes, O. M. Løvvik, and E. J. Baerends, J. Chem. Phys. **107**, 10 652 (1997).
- ³⁸M. Burgess and O. M. Løvvik (unpublished).